Machinability and properties of zirconia ceramics prepared by gelcasting method

Jaroslav Kastyl[a,*], Zdenek Chlup[b], Premysl Stastny[a], Martin Trunec[a, c]

[a]CEITEC BUT, Brno University of Technology, Brno, Czech Republic

[b]CEITEC IPM, Institute of Physics of Materials, Academy of Sciences of the Czech Republic, Brno, Czech Republic

[c]Institute of Materials Science and Engineering, Brno University of Technology, Brno, Czech Republic

*Corresponding author:
Central European Institute of Technology
Brno University of Technology
Purkynova 123, 612 00 Brno, Czech Republic
Phone: +420 541149710
e-mail: jaroslav.kastyl@ceitec.vutbr.cz
ORCID: 0000-0001-8145-604X

Abstract

The machinability of newly developed zirconia ceramics for CNC milling was investigated. The zirconia blanks were prepared by the gelcasting method and tested in the green and two pre-sintered states. All blanks exhibited uniform sintering shrinkage in all directions. The blanks were investigated from the viewpoint of surface milling roughness, quality of milled edges and sharp tips, and machinability of thin structures. The best milling results were obtained for the blanks pre-sintered at 900 °C/1 h. Mechanical properties of zirconia blanks, such as biaxial flexural strength, microhardness, indentation elastic modulus, and fracture toughness were determined in the green and pre-sintered states (900 °C/1 h and 1100 °C/1 h) and the

correlation with the milling results was discussed. The biaxial strength tests of sintered discs showed the advantage of optimized surface milling over conventional polishing.

Keywords: Zirconia; gelcasting; pre-sintering; machinability; CNC milling; mechanical properties

1. Introduction

The milling of ceramics in the pre-sintered state has been an important shaping method in dentistry for many years and is also suitable in other engineering areas such as prototype testing and low-series production of parts [1-5]. The machinable ceramic blanks are often produced as pre-sintered ceramic discs compacted by cold isostatic pressing [6-10]. Several processing problems are connected with these blanks. Namely non-uniform shrinkage during sintering, caused by non-uniform particle compaction during pressing or the choice of suitable pre-sintering temperature. Different shrinkage coefficients are provided directly by the manufacturers otherwise it must be verified in a laboratory. The non-uniform shrinkage of the blank can be solved during the CAD-CAM process but it brings additional difficulties [11-14]. An appropriate pre-sintering temperature ensures the required mechanical properties of the ceramic blanks [15, 16]. Sufficient hardness and strength are necessary for blank handling and milling but if these parameters are too high, they can detrimentally affect the quality of milled ceramics. The roughness of milled parts increases with higher pre-sintering temperatures [17]. Thus the choice of an appropriate pre-sintering heat treatment is critical. Another option is to mill the ceramic blanks in the green state, i.e. after the powder compaction before any heat treatment. Many studies were focused on the green milling, where the milling parameters such as the cutting speed, depth and width of cut [4, 9, 18-26] and surface roughness and strength [9, 27] of the green blanks were evaluated. Chipping and cracks formation are common failures

arising during milling and the quality of edges is also often used to characterise the blank machinability. It was reported that in the case of blanks fabricated by cold isostatic pressing a higher quality of sharp edges can be achieved in samples of a lower strength [28, 29].

The aim of this study was to investigate newly developed machinable zirconia blanks prepared by the gelcasting method and to determine the effect of different pre-sintering states of the blanks on their machinability and mechanical properties. The effect of the surface roughness of milled samples on their strength after sintering was investigated as well.

2. Experimental procedure

2.1. Materials and preparation of machinable blanks

Tetragonal zirconia powder (TZ-3YS-E, Tosoh, Japan) stabilized with 3 mol% of Y_2O_3 and a specific surface area of 6.8 m^2/g was used to prepare zirconia blanks by the gelcasting method. The zirconia powder was dispersed in a premix solution of monomers to obtain a suspension with a powder loading of 45 vol%. The premix monomer solution was prepared by dissolving 15 wt% of monomers in deionized water. Methacrylamide (109606, Sigma-Aldrich Chemie, Germany) and N, N´-methylene bisacrylamide (146072, Sigma-Aldrich Chemie, Germany) were used as the linear monomer and cross-linker, respectively. The ratio of the linear monomer to the cross-linking monomer was 4:1. A commercial dispersant (0.5 wt% with respect to the ceramic powder), Dolapix CE 64 (Zschimmer & Schwarz, Germany), was used to stabilize ceramic particles in the suspension. The ceramic suspension was ball-milled with 1 mm zirconia balls (YTZ, Nikkato-Tosoh, Japan) for 48 h. A 5% water solution of ammonium persulfate (215589, Sigma-Aldrich Chemie, Germany) was added to initiate the polymerization of dissolved monomers at room temperature [30]. The amount of ammonium persulfate was 0.175 wt% with respect to pure monomers in order to accomplish complete polymerization in

about 2 h. After the addition of the initiator, the ceramic suspension was immediately cast into the plastic moulds and gelled under nitrogen atmosphere. The zirconia bodies were removed from the moulds after gelation and dried in a climate box at 20 °C, with the relative humidity decreasing from 98 % to 60 % over a period of 168 h, followed by final drying under laboratory conditions. Zirconia blanks were pre-sintered at 900 and 1100 °C with a dwell of 1 h. The heating rate was 50 °C h^{-1} up to 500 °C and then 120 °C h^{-1} up to the pre-sintering temperature. Two types of disc-shaped ceramic blank were prepared with diameters of 30 and 40 mm and thicknesses of 5 and 10 mm, respectively.

2.2. CAD-CAM milling

Autodesk® Inventor® Professional 2018 with HSM Ultimate 2018 module was used to design the models and setup of milling paths, and to generate NC codes for the CNC milling machine (HWT E-442 CNC TROLL, AZK, Czech Republic). Two types of diamond-coated mills with end diameters of 2 mm and work lengths of 2 mm were used for the milling of ceramics blanks: a ball end mill (D-EPDB-2020-20 Epoch21, MMC Hitachi Tool Engineering Europe, Germany) and a flat end mill (D-EPDR-2020-20-02 Epoch21, MMC Hitachi Tool Engineering Europe, Germany) with a corner radius of 0.2 mm. The milling tools were checked for wear damage and they were replaced when any wear of the diamond coating was observed. All ceramic blanks were fastened using a vacuum table and before the milling tests they were first pre-milled in two steps to a default height using the flat end mill. A spiral strategy of milling to default heights of 4 mm and 8 mm for 30 mm and 40 mm discs, respectively, was employed. The milling parameters were following: the depth of cut a_p = 0.5 mm, and the width of cut a_e = 0.8 mm for initial roughening, and a_p = 0.1 mm and a_e = 0.8 mm for finishing in the last step. The spindle and feed speeds of 20 000 rpm and 600 mm min^{-1}, respectively, were used in all milling experiments. The models for milling experiments are shown in Fig. 1. The surface

This is an original manuscript of an article published by Taylor & Francis in Advances in Applied Ceramics on 11 Oct 2019, available online: https://doi.org/10.1080/17436753.2019.1675402

milling roughness (Fig. 1a), quality of milled edges and wedge tips (Fig. 1b), and machinability of thin structures (Fig. 1c) were tested. Details of the individual experiments will be specified later. All the milling experiments were carried out with zirconia blanks in three processing states: green (dried only), pre-sintered to 900 °C/1 h, and pre-sintered to 1100 °C/1 h.

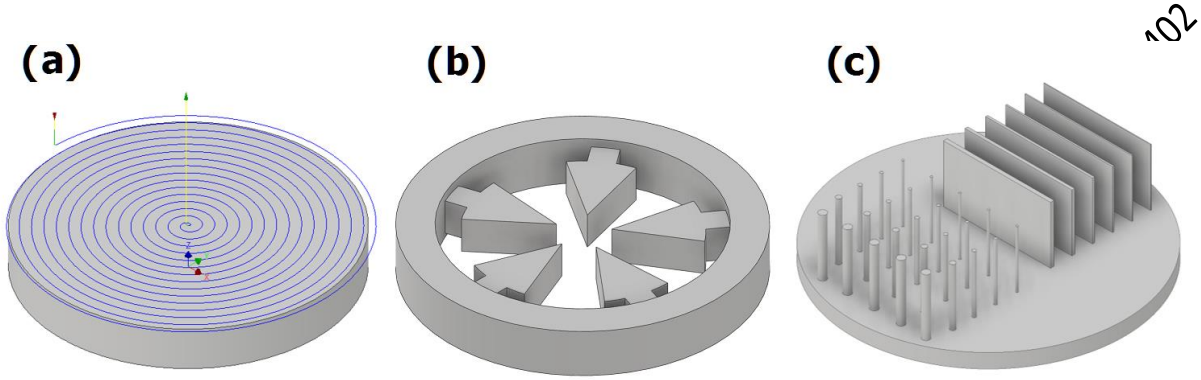

Fig. 1 Models designed for the milling experiments, showing a) spiral strategy on a flat disc for the surface roughness evaluation, b) wedges for the evaluation of edge and tip quality, and c) pins and lamellae for the evaluation of machinability of thin structures.

2.3. Post-milling processes and sintering

The milled surface of each sample was blown by low-pressure air in order to remove the ceramic dust after milling and the cleaned samples were sintered in an air atmosphere. The heating rate was 600 °C h^{-1} up to a temperature of 780 °C and then 300 °C h^{-1} up to a sintering temperature of 1450 °C with a dwell of 2 h at the sintering temperature. The samples milled in the green state (dried only) were pre-sintered to 800 °C before the final sintering schedule was applied.

2.4. Evaluation methods

The surface roughness of horizontal surfaces was investigated using a DektakXT stylus profilometer (Bruker Corporation, USA) according to EN ISO standards [31, 32]. The

profilometer tip radius 12.5 µm was used. The direction of the recorded roughness profile was always perpendicular to the toolpath direction. The data obtained by the profilometer were processed by the Gwyddion software [33] and the roughness parameters *Ra* (arithmetical mean deviation from the profile mean line) and *Rz* (average maximum peak to valley of five consecutive sampling lengths) were evaluated. The morphology of the milled surface and the milling defects were analysed using an electron scanning microscope (SEM) (Verios 460L, FEI, Czech Republic). The microhardness, HV 0.1, as well as the indentation elastic modulus, E_{IT}, were measured on the machined surface of milled discs prior to sintering in accordance with the EN ISO 6507 standard [34], using an instrumented hardness testing system Zwick Z2.5 equipped with the ZHU0.2 micro hardness head (Zwick/Roell, Germany). A minimum of 20 indents were used to calculate an average hardness. The fracture toughness values were determined using a universal testing machine (8862, Instron, USA) by the chevron notch beam (CNB) technique in the three-point bending configuration with a span of 16 mm and a crosshead speed of 5 µm min^{-1}. The fracture toughness values for CNB specimens were calculated using Blum's slice model [35]. A fractographic analysis was conducted on the fracture surfaces of broken specimens using SEM (Vescan Lyra 3 XMU, Czech Republic) to identify the acting fracture mechanisms for each treatment. The biaxial strength was determined using a universal testing machine (8862, Instron, USA) in the ball-on-3-balls biaxial bending configuration for green, pre-sintered and sintered ceramic discs (disc cast to 30 mm in diameter and milled to 4 mm in height) with supporting and loading ball diameter of 17.463 mm (giving a supporting circle diameter of approx. 20 mm). Loading at a crosshead speed of 0.5 mm min^{-1} was used. More details of the biaxial strength measurements can be found elsewhere [36]. The parameters of the Weibull strength distribution were calculated numerically, using the maximum likelihood method, in accordance with the EN 843-5 standard [37]. At least 20 valid strength values for each batch were statistically analysed.

This is an original manuscript of an article published by Taylor & Francis in Advances in Applied Ceramics on 11 Oct 2019, available online: https://doi.org/10.1080/17436753.2019.1675402

3. Results and discussion

3.1. Blank shrinkage

It is essential to know the sintering shrinkage of ceramic blanks before milling to correctly design the model dimensions of a milled part in order to obtain the required dimensions of the final sintered part. Three testing cubes with an edge of 7 mm were milled at different positions in a 40 mm disc and the sintering shrinkage in all directions was measured (see Fig. 2).

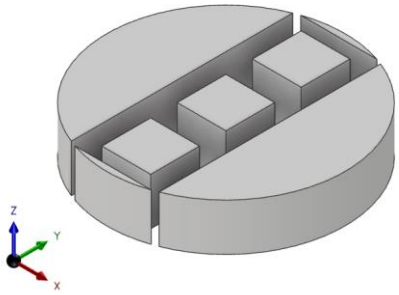

Fig. 2 Model designed for the milling of test cubes for shrinkage measurements.

A summary of the sintering shrinkage of the green and pre-sintered blanks is given in Table 1. As expected, the shrinkage decreased with increasing pre-sintering temperature. It is obvious from the results that the gelcast zirconia blanks exhibited a similar shrinkage not only at different positions in the blank but also in all directions. Thus the benefit from gelcast blanks for milling was verified and the shrinkage mismatch, common to pressed ceramic blanks [11, 12, 17, 30] was overcome.

Table 1 Shrinkage of ceramic blanks.

Pre-sintering state	Linear shrinkage* (%)		
	X	Y	Z
green	20.41 ± 0.25	20.47 ± 0.15	20.41 ± 0.05
900 °C/1 h	19.90 ± 0.12	19.94 ± 0.15	19.95 ± 0.19

1100 °C/1 h	18.90 ± 0.08	18.95 ± 0.12	19.04 ± 0.03

* An average value is given with the 95% confidence interval.

3.2. The surface roughness of milled discs

Spiral milling was used to obtain a flat horizontal surface, i.e. a milled surface oriented perpendicularly to the tool axis, on a pre-milled 30 mm disc (see Fig. 1a). The milling strategies applied are shown in Table 2.

Table 2 Milling strategies and cutting parameters for flat surfaces.

Milling strategy	Depth of cut a_p (mm)	Width of cut a_e (mm)
B-0.1-0.2	0.1	0.2
B-0.5-0.2	0.5	0.2
B-0.1-1.0	0.1	1.0
B-0.5-1.0	0.5	1.0
B-0.1+0.1-0.2 *	0.1+0.1	0.2
F-0.1-0.4	0.1	0.4
F-0.5-0.4	0.5	0.4
F-0.1-1.5	0.1	1.5
F-0.5-1.5	0.5	1.5
F-0.1+0.1-0.4 *	0.1+0.1	0.4

* Two layers with indicated depths of cut were removed in these strategies.

The strategy abbreviations specify the milling parameters. The first capital letter in the strategy abbreviation determines the type of the milling tool ("B" for the ball end mill and "F" for the flat end mill) and the two following numbers determine the depth of cut (a_p) and the width of cut (a_e). These milling strategies were applied to the green and pre-sintered blanks. The roughness of surfaces milled with different milling strategies was evaluated before and after sintering to determine the sintering effect on the roughness parameters. The samples after

sintering exhibited in most cases lower roughness than the samples measured before sintering. This is contrary to a recent study [39], where the commercially available zirconia discs were machined in a similar manner. It was reported that after sintering, the milled surfaces roughened due to an induced grain growth and phase transformation [17, 39]. In our case, the slight surface roughening, which was observed in only a few samples, was attributed rather to the sintering of milling debris on the surface than to grain coarsening and phase transformation.

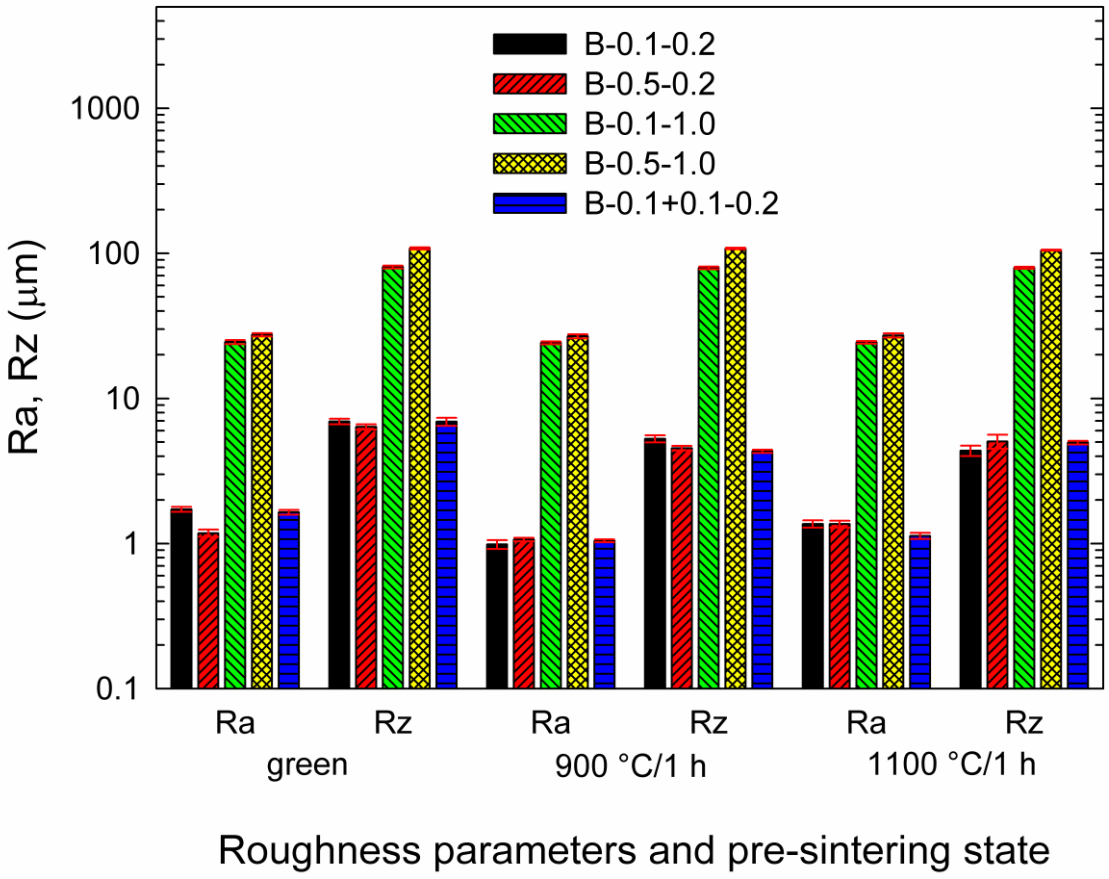

Fig. 3 Surface roughness parameters measured on sintered samples after milling with the ball end mill. The error bars show 95% confidence interval.

The roughness parameters measured on sintered samples after milling with the ball end mill are shown in Fig. 3. It is obvious that in the case of the ball end mill the surface roughness was mainly dependent on the width of cut. The increase in the width of cut from 0.2 to 1.0 mm

resulted in an increase in the roughness values by one order of magnitude. The depth of cut was less important. The lowest surface roughness (Ra = 0.9 µm and Rz = 3.9 µm) was achieved using the finest strategy (B-0.1-0.2) on the blank pre-sintered at 900 °C/1 h. Milling two layers with the fine strategy did not improve the roughness parameters. Milling the blank in the green state (dried only) provided slightly worse roughness than milling of the blank pre-sintered at 900 °C/1 h. However, short cracks appeared on the surface of the green blank after milling. These cracks were located perpendicularly to the direction of tool rotation and had a length of about 5 µm. They were regularly repeated with spacing of about 2 µm. Several cracks are highlighted by dashed lines in Fig. 4a. Surprisingly, the cracks visible before sintering disappeared after the sintering process (see Fig. 4b). Such cracks were not observed after milling with the flat end mill.

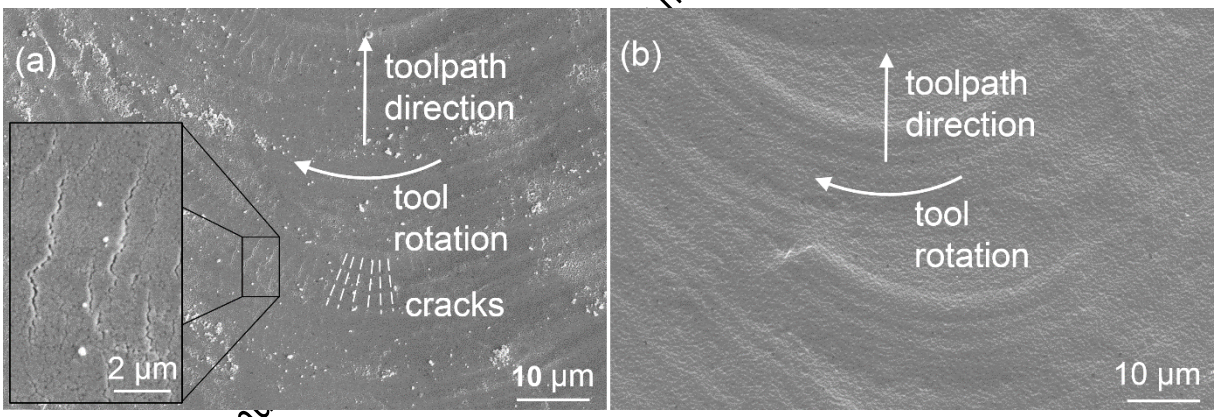

Fig. 4 SEM micrographs of a green blank milled with the B-0.1-0.2 strategy showing a) cracks on the milled surface (the detail of the cracks is shown in the inset) and b) defect-free surface of the same sample after sintering.

The roughness parameters measured on sintered samples after milling with the flat end mill are shown in Fig. 5. The roughness parameters after milling with the flat end mill were 1-2 orders of magnitude lower than the roughness parameters after milling with the ball end mill.

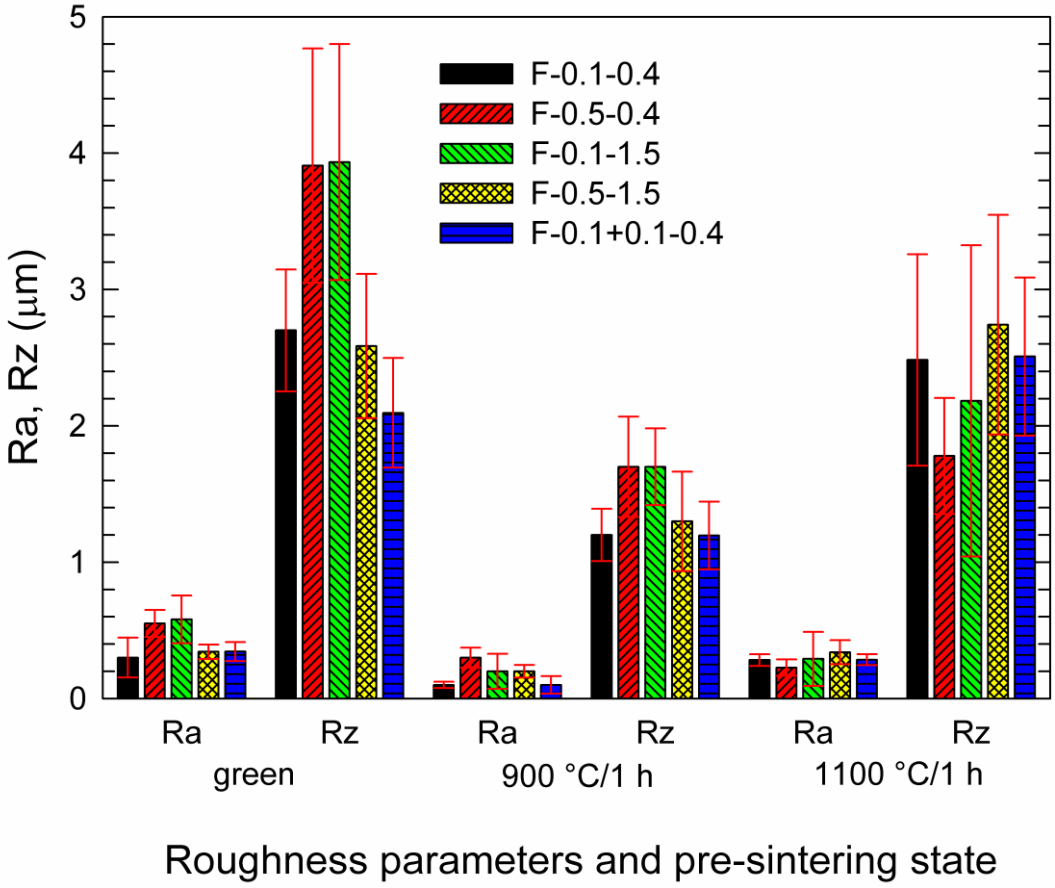

Fig. 5 Surface roughness parameters measured on sintered samples after milling with the flat end mill. The error bars show 95% confidence interval.

The effect of different strategies with the flat end mill on surface roughness was not very pronounced. The lowest surface roughness (*Ra* = 0.1 µm and *Rz* = 1.2 µm) was achieved using the finest milling strategy (F-0.1-0.4) on the blank pre-sintered at 900 °C/1 h. Similar to the ball end mill, milling two layers using the fine strategy with the flat end mill did not result in decreased roughness parameters. Milling with the flat end mill provided not only a much lower surface roughness than the ball end mill but it also took much less time to mill the surface. The lower milling time was the result of a larger width of cut and thus a shorter milling path. The calculated times for the tested milling strategies are given in Table 3. Although the flat end mill

is of limited use in the milling of complex parts with curved surfaces, it should be the preferred tool for large flat surfaces.

Table 3 Milling times of different milling strategies.

Strategy	Time (min:sec)	Strategy	Time (min:sec)
B-0.1-0.2 B-0.5-0.2	6:35	F-0.1-0.4 F-0.5-0.4	3:26
B-0.1-1.0 B-0.5-1.0	1:33	F-0.1-1.5 F-0.5-1.5	1:08
B-0.1+0.1-0.2	12:54	F-0.1+0.1-0.4	6:37

3.3. Quality of edges and tips

To study the quality and sharpness of milled edges and tips a model was designed (see Fig. 1b), where five wedges were milled using five selected strategies with the ball end mill. The wedges were 4 mm thick and had an edge of 9.7 mm. The radius of the wedge tip, r, and the maximum chipping distances on the wedge edges for both the tool entry side, H_E, and the tool exit side, H_X, were used to evaluate the quality of edges and tips for different blanks and milling strategies. Fig. 6 shows the evaluation criteria for the edge and tip quality. The results obtained on sintered bodies are summarized in Table 4.

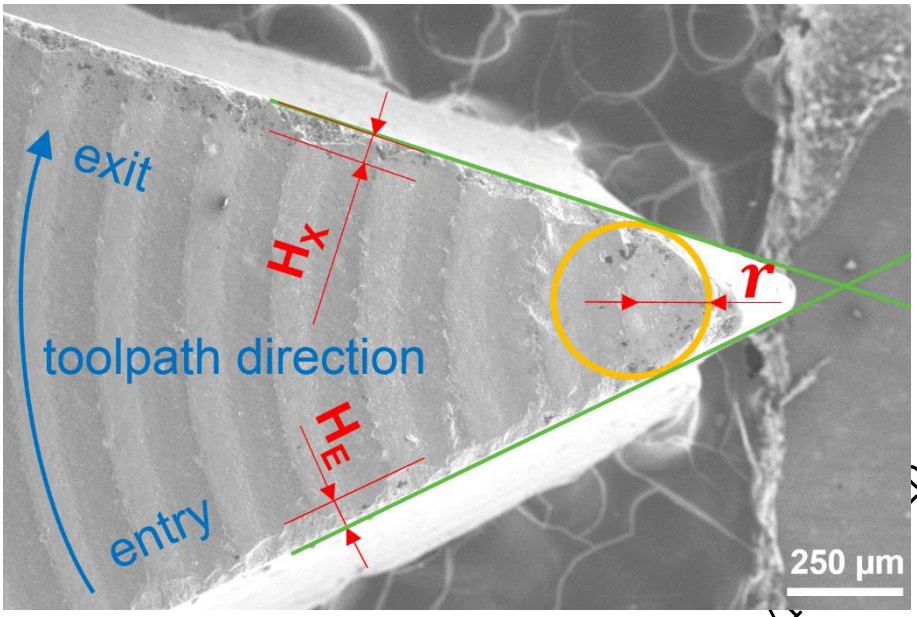

Fig. 6 Evaluation criteria for the edge and tip quality.

Table 4 Parameters evaluating the quality of milled edges and tips in sintered test bodies.

Strategy	Green			900 °C/1 h			1100 °C/1 h		
	r (µm)	H_E (µm)	H_X (µm)	r (µm)	H_E (µm)	H_X (µm)	r (µm)	H_E (µm)	H_X (µm)
B-0.1-0.2	129	116	85	71	42	184	66	0	41
B-0.5-0.2	161	160	86	349	147	80	160	198	100
B-0.1-1.0	249	81	68	482	199	0	55	0	0
B-0.5-1.0	133	66	342	141	66	64	89	49	50
B-0.25-0.25	199	88	68	116	0	0	73	120	33

The samples pre-sintered at 1100 °C/1 h exhibited the lowest radii of the milled wedge tips, i.e. the sharpest tips. The chipping on the edges was more random. Anyway, we can conclude from these experiments that the best quality of edges and tips was obtained for the blanks pre-sintered at 1100 °C/1 h and milled with strategies with a small depth of cut. Fig. 7 compares the SEM images of sintered wedges milled using the finest strategy (B-0.1-0.2) from a green blank and a blank pre-sintered at 1100 °C/1 h. Similar results were reported in [16], where the authors machined zirconia blanks prepared by die pressing. They achieved the best quality of edges in a sample pre-sintered at 1000 °C/4 h.

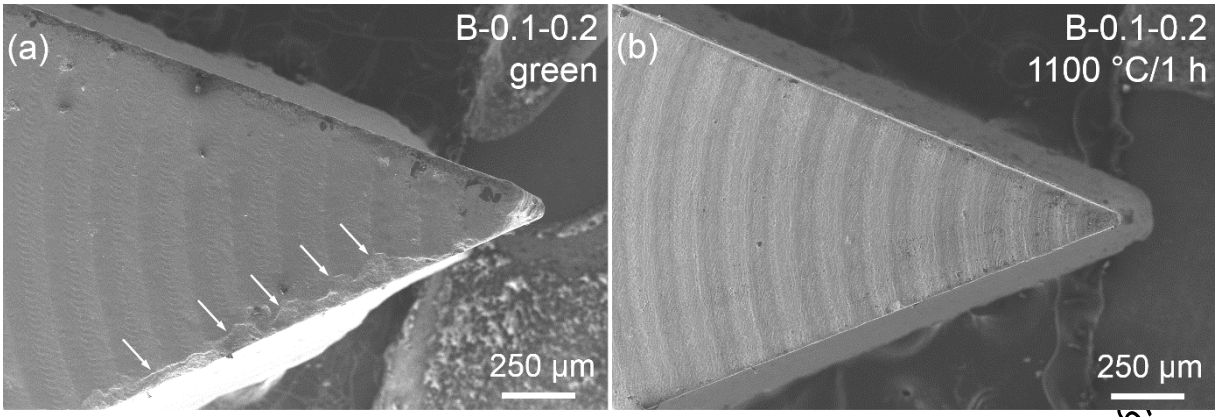

Fig. 7 SEM micrographs of wedges after the sintering of a) a sample milled in the green state (arrows indicate chipped areas) and b) a sample milled in the pre-sintered state (at 1100 °C/1 h).

3.4. Machinability of thin structures

For the verification of the machining possibilities of tested blanks, the pins (with a nominal diameter of 0.3, 0.4, 0.5, 0.7, and 1.0 mm) and lamellae (with a nominal thickness of 0.1, 0.15, 0.2, 0.3, 0.4, and 0.5 mm), all of them with a height of 6.5 mm, were machined by the B-0.5-0.2 strategy. The model of tested body is shown in Fig. 1c. It is clear from the comparison of milled samples (Fig. 8a) that the best results were obtained for the blank pre-sintered at 900 °C/1 h. All pins whose nominal diameter was 0.4 mm or higher were successfully machined. The thinnest lamella with a nominal thickness of 0.1 mm has small chipping defects on the edges. The sample milled from the blank pre-sintered at 1100 °C/1 h reached a similar result but not all the thinnest pins and lamellae were defect-free. The worst results were obtained for the blank in the green state, where only pins with a nominal diameter of 0.7 mm survived the milling and only the thickest lamella with a nominal thickness of 0.5 mm was defect-free. Sintered pins and lamellae are depicted in Fig. 8b. No visible deformations such as shape irregularities, cracks or pores were observed after sintering. This confirmed the uniform shrinkage of blanks in all directions during sintering as discussed earlier. The thinnest pins reached a diameter of 320 µm and the thinnest lamella thickness was 80 µm in the sintered sample milled from the blank pre-sintered at 900 °C/1 h, which is consistent with the shrinkage measurements (see Table 1).

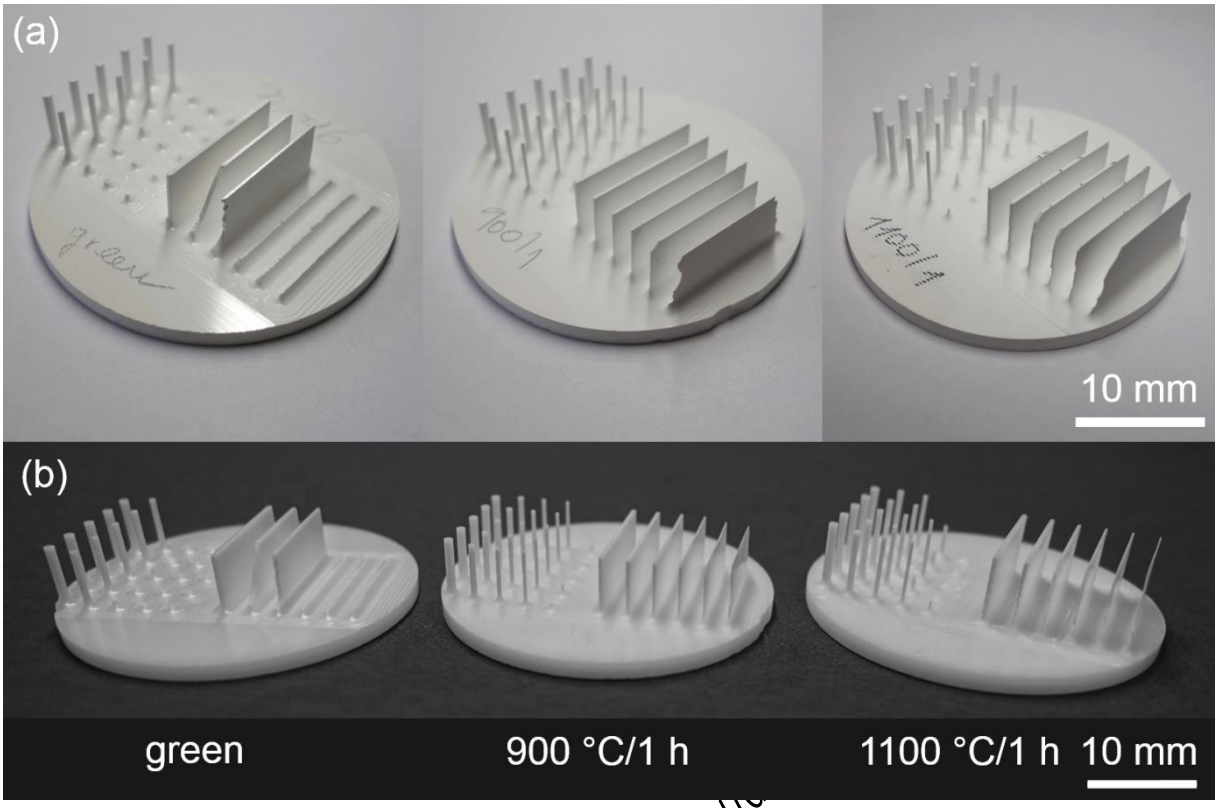

Fig. 8 Photographs of pins and lamellae a) as milled and b) after sintering.

3.5 Mechanical properties of blanks and sintered ceramics

The mechanical properties (hardness, flexural strength, fracture toughness, and Young's modulus) of green and pre-sintered blanks are compared in Fig. 9. It is evident from Fig. 9 that the blank providing the best milling behaviour, i.e. the blank pre-sintered at 900 °C/1 h, exhibited the lowest hardness, strength, elastic modulus, and fracture toughness. Similar results were found in [28], where the best machining properties were obtained for a compact of a relatively low strength in the pre-sintered state.

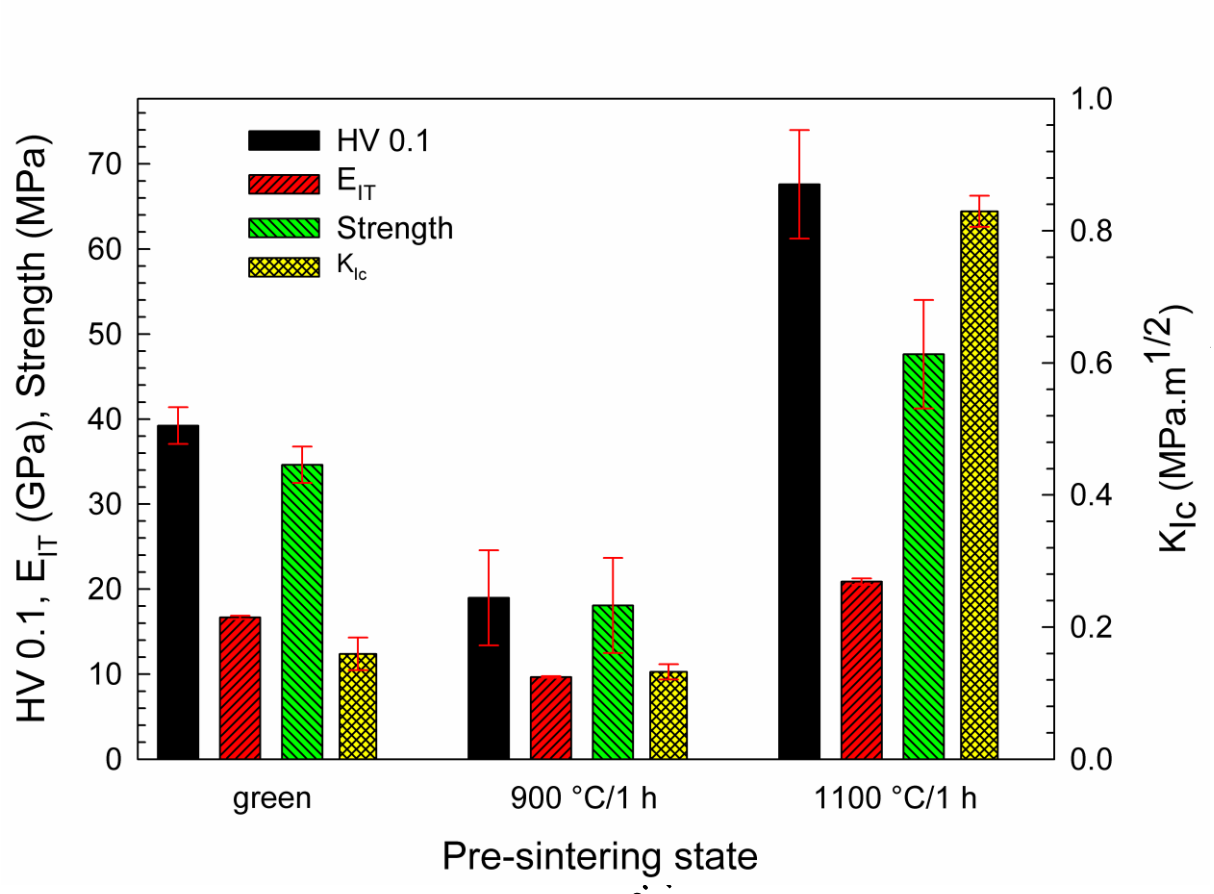

Fig. 9 Mechanical properties of green and pre-sintered blanks. The error bars show 95% confidence interval.

It is supposed that these low mechanical parameters of the blank led to the optimal cutting off process because only small fragments of the base material were removed, with a minimal damage zone formed in the surrounding material. The small damage zone was also supported by the low elastic modulus value. When the material was elastically loaded during the cutting process, the generated elastic stress field was acting only over a short distance. The microstructure of the material pre-sintered at 900 °C/1 h exhibits only partially joined (sintered) powder particles. However, the effect of the mechanical parameters on the milling behaviour of ceramic blanks must be more complex. The green blanks with mechanical properties being very close to the blanks pre-sintered at 900 °C/1 h provided the worst milling results, whereas the blank pre-sintered at 1100 °C/1 h with a much higher strength, hardness, and fracture

toughness provided a milling behaviour comparable to the best blank (900 °C/1 h). The composite structure of brittle polymer strongly connected to ceramic particles in the green blanks was probably responsible for the different mechanism of the material removal during milling compared with pre-sintered blanks, which resulted in a poor milling behaviour. We can conclude that the prediction of the milling behaviour of ceramic blanks from their mechanical properties is difficult and needs further extensive investigation.

The effect of the milled surface on biaxial strength of sintered samples was investigated on a sintered disc prepared by milling from blanks pre-sintered at 900 °C/1 h using the finest milling strategies B-0.1-0.2 and F-0.1-0.4, i.e. using strategies that provided the best surface roughness after milling with ball end mill and flat end mill, respectively. For comparison, the discs pre-milled to the default height (4 mm), sintered and diamond ground and polished down to 1 µm diamond emulsion were also tested. Two different polishing procedures with the 1 µm diamond emulsion were used. One set of discs (P1) was polished on a polishing cloth (MD-Dac, Struers, Czech Republic), the other set (P2) was polished on a composite disc (MD-Largo, Struers, Czech Republic). The surface topology of the test discs is shown in Fig. 10. The roughness parameters *Ra* and *Rz* of the milled samples after sintering have been discussed above. The roughness parameters of the polished sample groups P1 and P2 were identical. The *Ra* and *Rz* values were 0.02 ± 0.01 µm and 0.44 ± 0.21 µm, respectively.

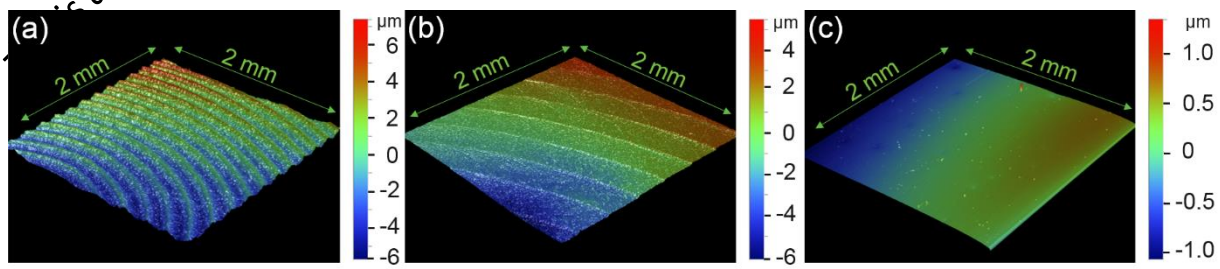

Fig. 10 Surface topography of sintered samples prepared from blanks pre-sintered at 900 °C/1 h by a) milling using the B-0.1-0.2 strategy, b) milling using the F-0.1-0.4 strategy and c) polishing (P1, P2). Please note the different colour scales

The effect of surface quality on the strength of sintered discs is obvious from Table 5. The Weibull plots of biaxial strength are given in Fig. 11. The polished samples exhibit a surprisingly high difference (nearly 170 MPa in the characteristic strength), even though the roughness was the same. The difference can only be explained by the formation of larger microcracks and subsurface damage due to the application of the polishing method P1. Both milled sample sets exhibited strength on a similar level, which lay between the samples polished by the methods P1 and P2.

Table 5 Mechanical properties of sintered zirconia discs

Sample	n	Mean biaxial strength	Weibull characteristics	
			Modulus m	Characteristic strength σ_0
	(-)	(MPa)	(-)	(MPa)
B-0.1-0.2	21	1054 ± 65	$13.95^{+2.95}_{-3.13}$	1116^{+73}_{-69}
F-0.1-0.4	20	1120 ± 43	$11.7^{+4.36}_{-4.62}$	1162^{+51}_{-50}
P1	40	990 ± 49	$6.57^{+1.67}_{-1.75}$	1056^{+58}_{-57}
P2	30	1153 ± 61	$7.20^{+2.15}_{-2.26}$	1224^{+71}_{-69}

The mean biaxial strength and Weibull parameters are given with 95% confidence interval.

The discs with the surface milled by flat end mill reached nearly the strength of the polished samples prepared by the method P2. This fact indicates that surface damage caused by this milling strategy is small enough to be healed during the sintering process to the level of the polished sample. Therefore, the fracture initiation origins are comparable when the presumption of the same resulting microstructure is accepted. The highest Weibull modulus for the F-0.1-0.4 strategy supports the previous presumption that small defects can be healed during the sintering process but when polished afterwards, new defects (in the form of microcracks) can be formed. Only a minor strength decrease was observed for milled samples with a higher roughness

(milled using the B-0.1-0.2 strategy) compared to samples with a lower roughness (milled using the F-0.1-0.4 strategy). The surface roughening by a milling strategy can be a possible way of incorporating a surface roughness requested for some applications (dental or surgical implants) without sacrificing the strength as reported for sand blasting or grinding after sintering [40,41]. The strength of our sintered gelcast zirconia ceramics was comparable or higher than the strength of sintered commercially available machinable zirconia discs with similar surface roughness [42].

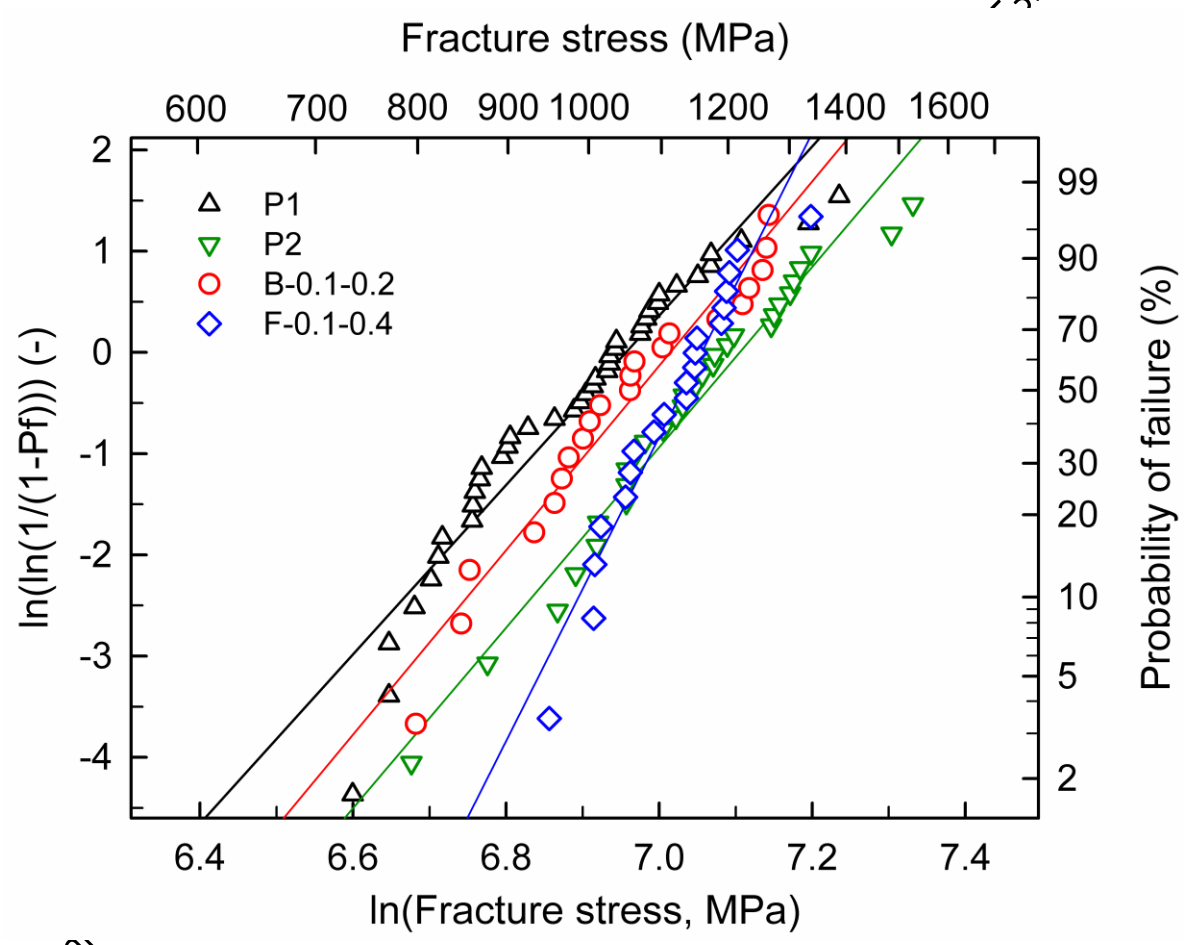

Fig. 11 Weibull plots of flexural strength of sintered samples milled with the ball end mill (B-0.1-0.2), flat end mill (F-0.1-0.4) and polished by different procedures (P1 and P2).

4. Conclusions

Machinable zirconia blanks of uniform shrinkage during sintering were successfully prepared by the gelcasting method. The gelcast blanks could be CNC milled not only in the pre-sintered states but also in the green state. The best milling results were achieved for blanks pre-sintered at 900 °C/1 h. The best surface roughness with the roughness parameters Ra = 0.1 μm and Rz = 1.2 μm was achieved on the sintered discs milled with the flat end mill. Thin structures were milled and sintered without observable distortions. Pins of 320 μm in diameter and lamellae of 80 μm in thickness, with both of them 5 mm high, were successfully manufactured. Among all the tested blanks, the blanks pre-sintered at 900 °C, i.e. blanks providing the best milling behaviour, exhibited the lowest strength, hardness, elastic modulus, and fracture toughness. The measurement of biaxial strength for sintered discs proved the advantage of milled surfaces compared with polished surfaces. The milled discs had comparable or higher biaxial strength than the polished samples and when milled with the flat end mill, they exhibited even a lower strength scatter.

Disclosure statement

No potential conflict of interest was reported by the authors.

Funding

This research was financially supported by the Ministry of Education, Youth and Sports of the Czech Republic under the project LTACH19034 and CEITEC 2020 (LQ1601). Part of the work was carried out with the support of the CEITEC Nano Research Infrastructure (MEYS CR, 2016-2019).

ORCID

Jaroslav Kastyl http://orcid.org/0000-0001-8145-604X

Zdenek Chlup http://orcid.org/0000-0002-6117-240X

Martin Trunec http://orcid.org/0000-0001-6402-7518

References

[1] P. Tidehag, Z. Shen, Digital dentistry calls the change of ceramics and ceramic processes, Advances in Applied Ceramics 118(1-2) (2019) 83-90.

[2] J. Han, J. Zhao, Z. Shen, Zirconia ceramics in metal-free implant dentistry, Advances in Applied Ceramics 116(3) (2017) 138-150.

[3] Y. Zhang, J.-m. Han, G. Zheng, H. Lin, W. Bai, J. Zhao, Z. Shen, Fatigue behaviours of the zirconia dental restorations prepared by two manufacturing methods, Advances in Applied Ceramics 116(7) (2017) 368-375.

[4] T. El-Wardany, R. Barth, J. Holowczak, W. Tredway, L.J. Chen, Optimum process parameters to produce green ceramic complex parts, CIRP Annals - Manufacturing Technology 58(1) (2009) 109-112.

[5] R. Janssen, S. Scheppokat, N. Claussen, Tailor-made ceramic-based components—Advantages by reactive processing and advanced shaping techniques, Journal of the European Ceramic Society 28(7) (2008) 1369-1379.

[6] R. Belli, M. Wendler, D. de Ligny, M.R. Cicconi, A. Petschelt, H. Peterlik, U. Lohbauer, Chairside CAD/CAM materials. Part 1: Measurement of elastic constants and microstructural characterization, Dental Materials 33(1) (2017) 84-98.

[7] H.J. Conrad, W.-J. Seong, I.J. Pesun, Current ceramic materials and systems with clinical recommendations: A systematic review, The Journal of Prosthetic Dentistry 98(5) (2007) 389-404.

[8] S.J. Ha, B.C. Shin, M.W. Cho, K.J. Lee, W.S. Cho, High speed end-milling characteristics of pre-sintered Al2O 3/Y-TZP ceramic composites for dental applications, Journal of the Ceramic Society of Japan 118(1383) (2010) 1053-1056.

[9] A. Malgarido, B.M. Purquerio, C.R. Foschini, C.A. Fortulan, Influence of the green-machining parameters on the mechanical properties of alumina rods, The International Journal of Advanced Manufacturing Technology 88(9) (2017) 3475-3484.

[10] A. Demarbaix, E. Rivière-Lorphèvre, F. Ducobu, E. Filippi, F. Petit, N. Preux, Behaviour of pre-sintered Y-TZP during machining operations: Determination of recommended cutting parameters, Journal of Manufacturing Processes 32 (2018) 85-92.

[11] G. Bukvic, L.E.d.A. Sanchez, C.A. Fortulan, A.A. Fiocchi, I.D. Marinescu, GREEN MACHINING ORIENTED TO DIMINISH DENSITY GRADIENT FOR MINIMIZATION OF DISTORTION IN ADVANCED CERAMICS, Machining Science and Technology 16(2) (2012) 228-246.

[12] M.g. Holthaus, S. Twardy, J. Stolle, O. Riemer, L. Treccani, E. Brinksmeier, K. Rezwan, Micromachining of ceramic surfaces: Hydroxyapatite and zirconia, Journal of Materials Processing Technology 212(3) (2012) 614-624.

[13] J. Kunii, Y. Hotta, Y. Tamaki, A. Ozawa, Y. Kobayashi, A. Fujishima, T. Miyazaki, T. Fujiwara, Effect of Sintering on the Marginal and Internal Fit of CAD/CAM-fabricated Zirconia Frameworks, Dental Materials Journal 26(6) (2007) 820-826.
[14] F. Beuer, J. Schweiger, D. Edelhoff, Digital dentistry: an overview of recent developments for CAD/CAM generated restorations, Br Dent J 204(9) (2008) 505-511.
[15] E.D. Case, F. Ren, P. Kwon, C.K. Kok, R. Rachedi, B. Klenow, Machining and Ceramic/Ceramic Joining to Form Internal Mesoscale Channels, International journal of applied ceramic technology 1(1) (2004) 95-103.
[16] H.W. Shin, E.D. Case, P. Kwon, F. Ren, C.K. Kok, Machining and Joining to form Internal MESO-Scale Channels in Ceramic Oxides, 27th Annual Cocoa Beach Conference on Advanced Ceramics and Composites: B: Ceramic Engineering and Science Proceedings (2003) 573-582.
[17] I. Denry, J.R. Kelly, State of the art of zirconia for dental applications, Dental Materials 24(3) (2008) 299-307.
[18] P. Dadhich, P.K. Srivas, S. Mohanty, S. Dhara, Microfabrication of green ceramics: Contact vs. non-contact machining, Journal of the European Ceramic Society 35(14) (2015) 3909-3916.
[19] S.D. Nunn, G.H. Kirby, Green machining of gelcast ceramic materials, April 1, 1996; Tennessee. (digital.library.unt.edu/ark:/67531/metadc668726/: accessed May 10, 2017), University of North Texas Libraries, Digital Library, digital.library.unt.edu; crediting UNT Libraries Government Documents Department. (1996).
[20] M. Desfontaines, Y. Jorand, M. Gonon, G. Fantozzi, Characterisation of the green machinability of AlN powder compacts, Journal of the European Ceramic Society 25(6) (2005) 781-791.
[21] R. He, R. Zhang, X. Zhu, K. Wei, Z. Gui, Y. Pei, D. Fang, Improved Green Strength and Green Machinability of ZrB2–SiC Through Gelcasting Based on a Double Gel Network, Journal of the American Ceramic Society 97(8) (2014) 2401-2404.
[22] G. Bukvic, A. Fiocchi, L. Sanchez, B. Purquerio, C. Fortulan, Influence of ceramic binders on mechanical properties and finishing of green machined alumina, 22nd International Congress of Mechanical Engineering (COBEM 2013), 2013.
[23] S.H. Ng, J.B. Hull, J.J. Henshall, Machining of novel alumina/cyanoacrylate green ceramic compacts, Journal of Materials Processing Technology 175(1–3) (2006) 299-305.
[24] R.K. Kambo, S. Dhara, P. Bhargava, Machining behaviour of green gelcast ceramics, Journal of the European Ceramic Society 23(7) (2003) 1005-1011.
[25] B. Su, S. Dhara, L. Wang, Green ceramic machining: A top-down approach for the rapid fabrication of complex-shaped ceramics, Journal of the European Ceramic Society 28(11) (2008) 2109-2115.
[26] S. Mohanty, A.P. Rameshbabu, S. Mandal, B. Su, S. Dhara, Critical issues in near net shape forming via green machining of ceramics: A case study of alumina dental crown, Journal of Asian Ceramic Societies 1(3) (2013) 274-281.
[27] S. Dhara, B. Su, Green Machining to Net Shape Alumina Ceramics Prepared Using Different Processing Routes, International Journal of Applied Ceramic Technology 2(3) (2005) 262-270.
[28] I. Birkby, G.P. Dransfield, P. McColgan, J.H. Song, J.R.G. Evans, FACTORS AFFECTING THE MACHINABILITY OF FINE CERAMIC POWDER COMPACTS, British Ceramic Transactions 93(5) (1994) 183-186.
[29] J.H. Song, J.R.G. Evans, On the machinability of ceramic compacts, Journal of the European Ceramic Society 17(14) (1997) 1665-1673.

[30] O. Bera, M. Trunec, Optimization of Fine Alumina Gelcasting Using In Situ Dynamic Rheology, Journal of the American Ceramic Society 95(9) (2012) 2849-2856.
[31] EN ISO 4287:1997, Geometrical Product Specifications (GPS) - Surface texture: Profile method - Terms, definitions and surface texture parameters, Geneva: International Organisation for Standardization, 1998.
[32] EN ISO 4288:1998, Geometric Product Specifications (GPS) - Surface texture: Profile method - Rules and procedures for the assessment of surface texture, Geneva: International Organisation for Standardization, 1998.
[33] Gwyddion software (GNU GPL license), version 2.49, http://gwyddion.net/.
[34] ISO 6507-1:2005, Metallic materials — Vickers hardness test — Part 1: Test method, Geneva: International Organisation for Standardization, 2005.
[35] I. Dlouhy, M. Holzmann, J. Man, L. Valka, The use of chevron notched specimen for fracture toughness determination, 1994.
[36] A. Börger, P. Supancic, R. Danzer, The ball on three balls test for strength testing of brittle discs: stress distribution in the disc, Journal of the European Ceramic Society 22(9) (2002) 1425-1436.
[37] ENV 843-5:1995, Advanced technical ceramics - Monolithic ceramics- Mechanical tests at room temperature - Part 5: Statistical analysis. Brussels: CEN, November 1996. 41 s.
[38] T.-H. Lan, C.-H. Wang, K.-K. Chen, M.-C. Wang, H.-F. Lee, Milling properties of low temperature sintered zirconia blocks for dental use, Materials Science and Engineering: C 73 (2017) 692-699.
[39] A.-R. Alao, R. Stoll, X.-F. Song, T. Miyazaki, Y. Hotta, Y. Shibata, L. Yin, Surface quality of yttria-stabilized tetragonal zirconia polycrystal in CAD/CAM milling, sintering, polishing and sandblasting processes, Journal of the Mechanical Behavior of Biomedical Materials 65 (2017) 102-116.
[40] Y. Zhang, B.R. Lawn, E.D. Rekow, V.P. Thompson, Effect of sandblasting on the long-term performance of dental ceramics, Journal of Biomedical Materials Research Part B: Applied Biomaterials 71B(2) (2004) 381-386.
[41] Y. Zhang, B.R. Lawn, Fatigue sensitivity of Y-TZP to microscale sharp-contact flaws, Journal of Biomedical Materials Research Part B: Applied Biomaterials 72B(2) (2005) 388-392.
[42] J. Hjerppe, T.O. Närhi, P.K. Vallittu, L.V.J. Lassila, Surface roughness and the flexural and bend strength of zirconia after different surface treatments, The Journal of Prosthetic Dentistry 116(4) (2016) 577-583.